

## Efficient photocathode performance of Lithium ions doped LaFeO<sub>3</sub> nanorod array for hydrogen evolution

Yang Li,<sup>a</sup> Tao Wang,<sup>\*a</sup> Bin Gao,<sup>a</sup> Xiaoli Fan,<sup>b</sup> Hao Gong,<sup>a</sup> Hairong Xue,<sup>a</sup> Songtao Zhang,<sup>c</sup> Xianli Huang,<sup>a</sup> Jianping He,<sup>\*a</sup>

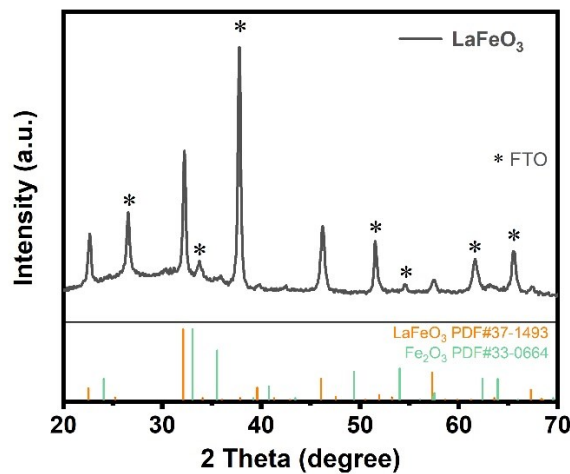


Figure S1. XRD pattern of LaFeO<sub>3</sub> film.

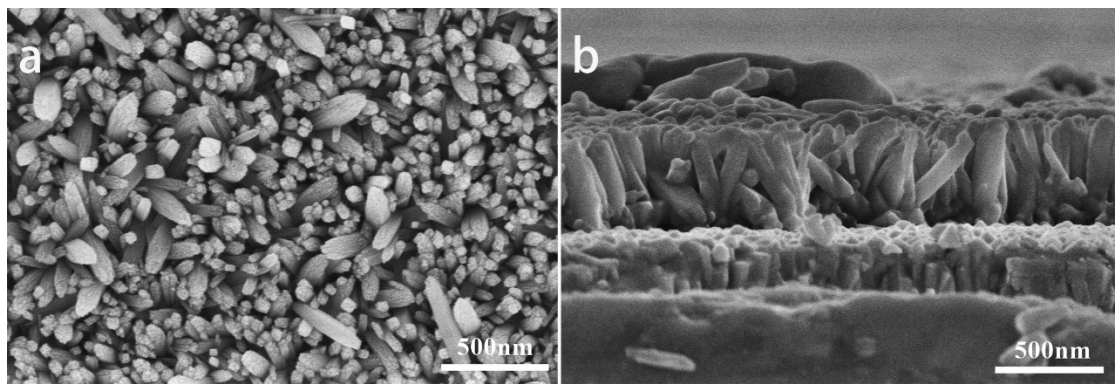


Figure S2. The top-view SEM images (a) and cross-view SEM (b) of  $\beta$ -FeOOH.

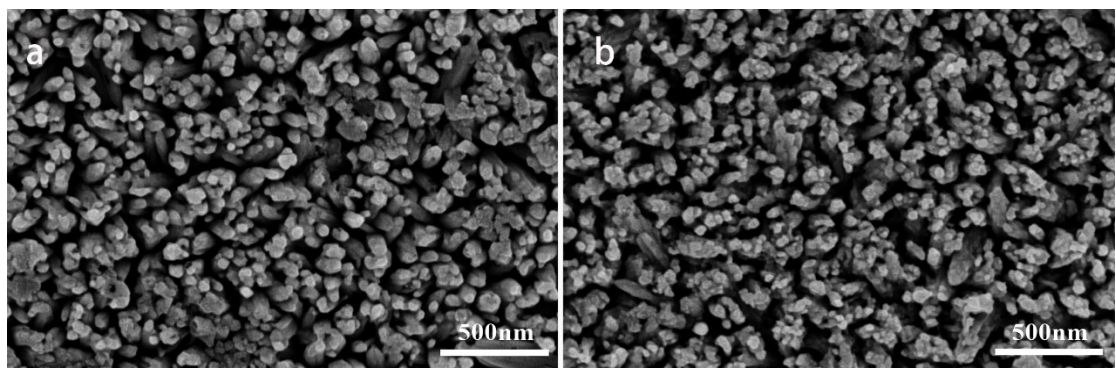


Figure S3. The top SEM images of (a) Li-LFO-1 and (b) Li-LFO-3.

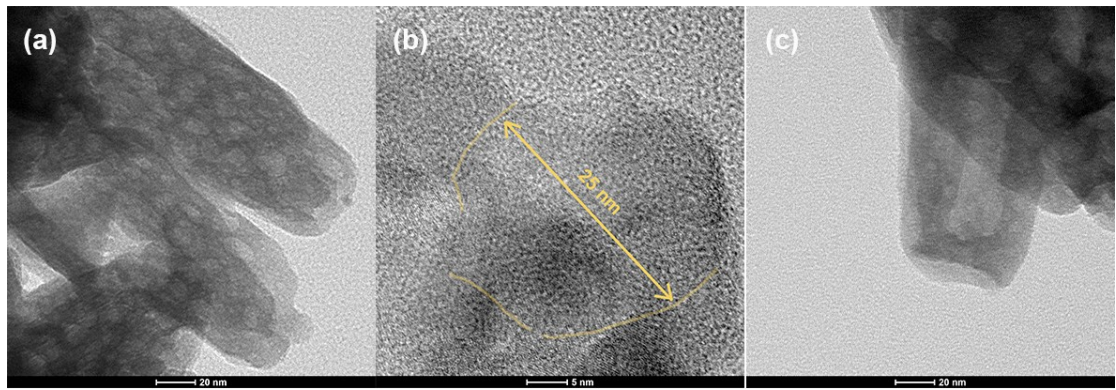


Figure S4. The HR-TEM images of (a)(b) pristine LaFeO<sub>3</sub> and (c) Li-doped LaFeO<sub>3</sub>.

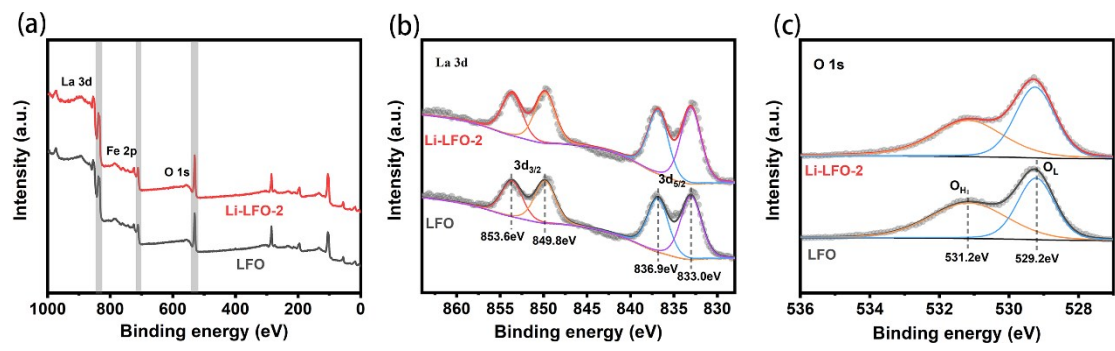


Figure S5. XPS survey spectra (a) and high-resolution of La 3d (b), O 1s (c).

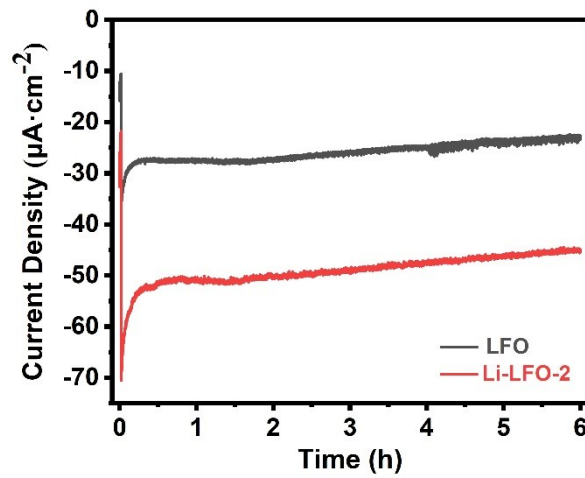


Figure S6. The chopped I-t curves at 0.4V vs. RHE for pristine and Li-doped LaFeO<sub>3</sub> for water reduction with N<sub>2</sub> bubbling.

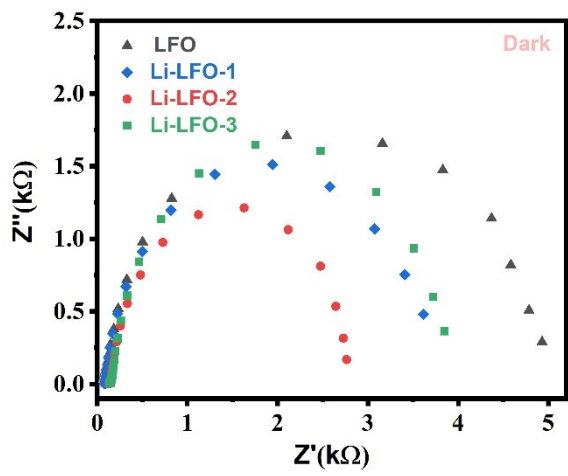


Figure S7. The EIS curves in light of pristine and Li-doped LaFeO<sub>3</sub> photocathodes measured in a solution saturated with O<sub>2</sub>.

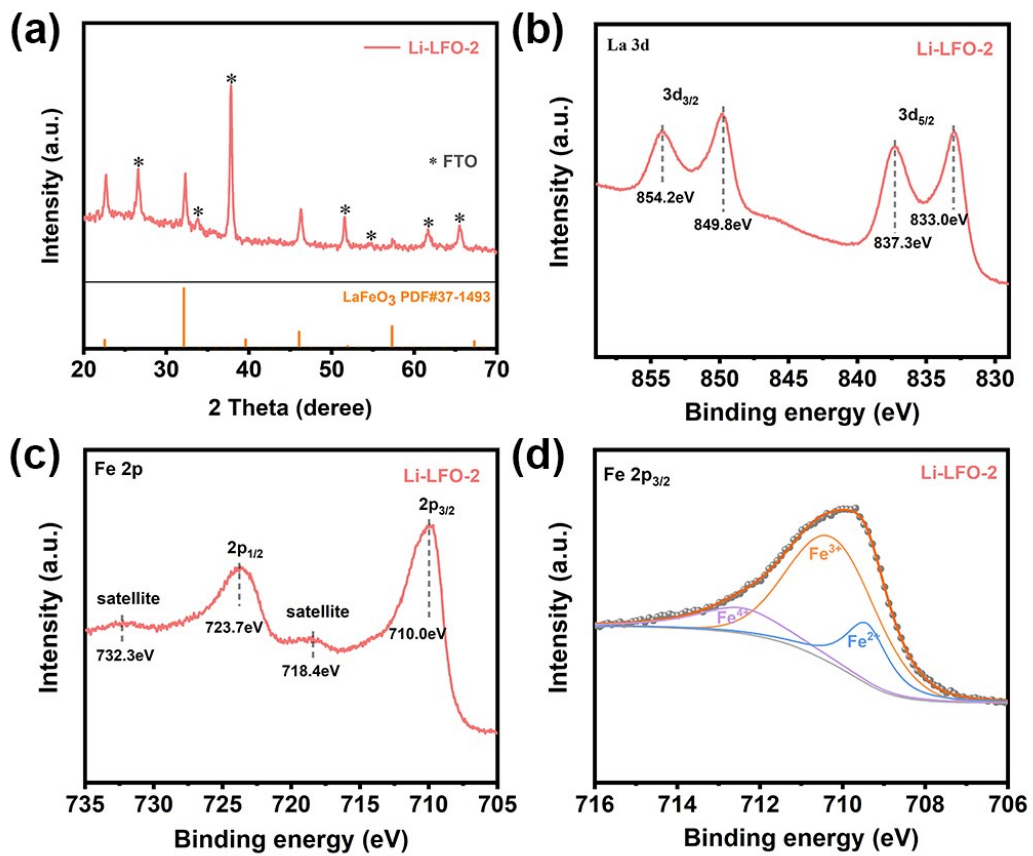


Figure S8. (a) XRD spectra, (b) XPS high-resolution spectra of La 3d, (c) XPS high-resolution spectra of Fe 2p and (d) peak fitting of Fe 2p<sub>3/2</sub> of Li-LFO-2 photocathode.

Table S1. The crystallite size calculated based on XRD information

<b>hkl</b>	<b>2θ(°)</b>	<b>β(rad)</b>	<b>D (nm)</b>	<b>Average crystallite size</b>
(101)	22.660	0.380	22.34	
(121)	32.240	0.326	26.58	
(202)	46.200	0.448	20.20	
(240)	57.539	0.493	19.26	

$$D_{hkl} = \frac{K\lambda}{\beta \frac{\pi}{180} \cdot \cos \theta}$$

Debye-Scherrer :

$D_{hkl}$  is the grain diameter perpendicular to the crystal plane (hkl) direction. K is the Scherrer constant, and  $K = 0.943$  (*cube grain*) .  $\lambda$  is the incident X-ray wavelength, and  $\lambda = 0.15406 \text{ nm}$  (*Cu K}\alpha*) .  $\theta$  is the Bragg diffraction angle.  $\beta$  is the half-width of the diffraction peak.

Table S2. LiNO<sub>3</sub> drop-cast solution concentrations and percentages of Lithium in the LaFeO<sub>3</sub> film

concentration of Li in drop-cast solution	atomic % of Li in LaFeO <sub>3</sub>
0.5 mM	0.75%
1.0 mM	3.8%
1.5 mM	5.7%

Table S3. The photocurrents of the LaFeO<sub>3</sub> photocathodes for PEC water reduction in the literature.

Photocathode and modification	Preparation	Potential	Current density	Reference
LaFeO <sub>3</sub>	Electrodeposition	0.4 V (vs. RHE)	-10μA·cm <sup>-2</sup>	1
LaFeO <sub>3</sub>	magnetron sputtering	0 V (vs. RHE)	-25μA·cm <sup>-2</sup>	2
(NiP+P1*)@ LaFeO <sub>3</sub>	spray pyrolysis	0.6 V (vs. RHE)	-20μA·cm <sup>-2</sup>	3
Au/ LaFeO <sub>3</sub>	sol-gel	0.6 V (vs. RHE)	-20μA·cm <sup>-2</sup>	4
Ni-LaFeO <sub>3</sub>	spray pyrolysis	0.6 V (vs. RHE)	-66μA·cm <sup>-2</sup>	5
Li- LaFeO <sub>3</sub>	Hydrothermal template method	0.4 V (vs. RHE)	-50μA·cm <sup>-2</sup>	This work

## Reference

- [1] G. P. Wheeler, V. U. Baltazar, T. J. Smart, A. Radmilovic, Y. Ping, K. S. Choi, *Chem. Mater.*, 2019, **31**, 5890-5899.
- [2] M. K. Son, H. Seo, M. Watanabe, M. Shiratani, T. Ishihara, *Nanoscale*, 2020, **12**, 9653-9660.
- [3] F. Li, R. Xu, C. Nie, X. Wu, P. Zhang, L. Duan, L. Sun, *Chem. Commun.*, 2019, **55**, 12940-12943
- [4] P. Wang, Y. He, Y. Mi, J. Zhu, F. Zhang, Y. Liu, Y. Yang, M. Chen, D. Cao, *RSC Adv.*, 2019, **9**, 26780-26786
- [5] G. S. Pawar, A. Elikkottil, B. Pesala, A. A. Tahir, T. K. Mallick, *Int. J. Hydrot. Energy*, 2019, **44**, 578-586